

The MRI Imaging of Cerebral Cavernous Malformation With Practical Use of Diffusion Weighted Image

Nobukata Kazawa, Yuta Shibamoto

Nobukata Kazawa, Yuta Shibamoto, Department of Radiology, Nagoya City University Hospital, 1 Kawasumi Mizuho Mizuho Ward, Nagoya City, Aichi prefecture, 467-0061, Japan

Correspondence to: Nobukata Kazawa, MD PhD, Department of Radiology, Nagoya City University Hospital, 1 Kawasumi Mizuho Mizuho Ward, Nagoya City, Aichi prefecture, 467-0061, Japan

Email: nobukaz@med.nagoya-cu.ac.jp

Telephone: + 81-052-853-8276

Received: March 14, 2015 Revised: April 10, 2015

Accepted: April 19, 2015

Published online: June 2, 2015

© 2015 ACT. All rights reserved.

Key words: Cerebral cavernous malformation; Diffusion weighted image; Intratumoral hemorrhage; Signal Intensity; Magnetic resonance image

Kazawa N, Yuta Shibamoto. The MRI Imaging of Cerebral Cavernous Malformation With Practical Use of Diffusion Weighted Image. *International Journal of Radiology* 2015; 2(1): 24-28 Available from: URL: <http://www.ghrnet.org/index.php/ijr/article/view/1108>

ABSTRACT

AIM: To evaluate the significance of diffusion weighted image(DWI) of the cerebral cavernous malformation in clinical practice.

MATERIALS AND METHODS: Thirty patients with 66 lesions (multiple 5 cases) were included in this study. The signal, configuration, anatomical location, size, and the number on each T1WI, T2WI, FLAIR, T2WI*, DWI, Gd (gadolinium)-T1WI, and the sequential signal change of DWI(central and peripheral area in cavernoma) were recorded.

RESULTS: The cerebral cavernous malformation (CCM) shows the signal of various phase of hematoma (hemorrhage) on both T1WI and T2WI MRI. On the diffusion weighted imaging (DWI), they showed the marked low (43.3%) and mixed high and low signal intensity (33.3%) even if they were very small appearing as areas of decreased signal (black dots) on T2WI. The low intense signal area on DWI assumed to reflect the hemosiderin or susceptibility effect and blood oxygen level dependent (BOLD) effect by the deoxyhemoglobin and T2 black out effect. The transient high signal foci on DWI were observed in 2(6.7%) cases in whom the intratumoral (re)hemorrhage were suspected.

CONCLUSIONS: The CCM tends to exhibit almost low signal intensity on DWI. DWI is a useful method like T2*WI and SWI for the detection of the tiny CCM.

INTRODUCTION

The cerebral cavernous malformation (CCM) is thought to be congenital abnormality of the cerebral vessels that affect 0.5% to 0.7% of the population^[1,2]. It occurs in two forms: a sporadic form characterized by isolated lesions, and a familial form characterized by multiple lesions with an autosomal dominant mode of inheritance. As compared with computed tomography (CT) and angiography, magnetic resonance imaging (MRI) was more sensitive in detecting cerebral cavernous malformations. Therefore, MRI is the most reliable clinical choice for the identification and follow-up of cavernous malformation. On T2-weighted image of MRI, the combination of a reticulated core of mixed high and low signals with a surrounding rim of low intensity suggests the diagnosis of a cavernous malformation. In the clinical practice, DWI (diffusion weighted image) is a very useful pulse sequence for the diagnosis of cerebral vascular disease including acute infarction or tumor characteristics. It is ultrasensitive to the motion of water protons and can detect ischemic lesions as early as 15 minutes after an occlusion of artery. This is the first study evaluating the usefulness of DWI of cerebral cavernous malformations (cavernoma).

MATERIAL AND METHODS

In order to elucidate the characteristics of brain CCM on MRI

imaging, consecutive 30 patients of 2 institutions were evaluated. The mean age was 53.4±13.5 years (mean±SD), with a range of 23 to 87 years. In which open surgical biopsies were performed on 3 cases, and the total 66 lesions (multiple 5 cases) diagnosed by the CT/MRI with the clinical course were included in this study. We excluded the tiny lesions smaller than 1mm in diameter or bright high intensity spot only on T1WI, because we can not rule out the calcified lesions, micro bleed scar, slow flow, stagnation or thrombosis of varying time course. The examinations were performed from August 2007 to March 2011 at Yoshikawa Hospital (n=15), and from April 2011 to December 2014 at NCU (Nagoya City University) Hospital (n=15). In both institutions, MRI were scanned by the same 1.5 Tesla supermagnetic unit [Intera Achieva(Philips Best Netherland)]. The IRB (Institutional Review Board) approval and the informed consent of each patients were obtained in each institutions. The pulse sequences and parameters were as follows; plain and gadolinium-DTPA enhanced T1WI [TR/TE=600 msec/20msec flip angle (FA) 69 degree], T2WI (TR/TE=3000/100 FA 90), fluid-attenuated inversion recovery (FLAIR) (TR/TE=6000/100 FA 90 IR 2000). DWI (TR/TE/TI=3125-5050/70/230 FA 90, b=1000s/m²) and, GRE- T2* (T2* SENSE TR/TE=600/20 FA 15) (slice thickness 5mm 1mm gap) or EPI-T2* WI (TR/TE=1071.2/14.148 FA 90) were scanned in all patients. The DWI signal and sequential change were also evaluated on all lesions. Susceptibility weighted imaging (SWI TR/TE=28/20, FA 15 acquisition matrix 384×202) were scanned in 12 lesions of 9 patients mainly due to the restriction of the scan time. Plain time-of-flight (TOF) MR angiography (TR/TE=17/6904 FA 20.1.2mm space gap 0.6mm) were scanned in 15 cases, CT(MDCT) (slice thickness 5-7mm) examinations were also performed in 15 lesions of 9 cases. The signal, configuration, anatomical location, size, and number on each T1WI, T2WI, FLAIR, T2WI*, DWI, Gd (gadolinium) enhanced -T1WI, SWI and their sequential signal changes, especially DWI were recorded.

RESULTS

The site of the lesions were as follows; medulla oblongata 1, medulla/pons 2, pons 3, midbrain/pons 1, middle brain 3, cerebellum 18, thalamus 4, internal capsule 2, basal ganglia 6, frontal lobe 10, parietal lobe 6, temporal lobe 6, occipital lobe 4 (Table 1). In cerebral parenchyma, almost all lesions were located in the deep white matter or subcortical white matter measuring about 4mm- to 23×19×17mm (mean 8.4mm) in diameter. The so-called mass effect (peri-tumoral edema) were only seen in 3 cases (5.2%). The hemorrhage perforated to the aqueduct of midbrain and subarachnoid hemorrhage was observed in each one case. On T1WI, they showed low (n=10), slightly low-iso (n=24), high and low mixed (n=16), high (n=16) intensity. On T2WI, they exhibited low (n=30), mixed (n=27) (Figure 1, 2), slightly high (n=4) and very high (n=5) signal intensities. T2WI low intensity rim (Figure 1) and permeative peripheral low signal area outside the tumor were observed in 30 (45%) and 5 lesions (7.6%). On FLAIR images, they exhibited indistinct (n=8), low (n=24), mixed (n=31) (Figure 2), and high (n=3) signal intensities. On T2WI* indistinct (n=10), low (n=34), mixed (n=19), and high (n=3) signal intensities were observed. On the diffusion weighted imaging (TR/TE/FA=3125-5050/70/90. b=1000sec/mm²), they showed indistinct (n=3, 10%), marked low intensity (n=13, 43.3%) (Figure 1), mixed high and low intensity [n=10, 33.3% (central high and peripherally low=6, 20%)], high intensity (n=2, 6.7%) (Table 2). In both 2 cases, transient high signal were observed in which we suspected intral-lesional hemorrhage (Figure 2).

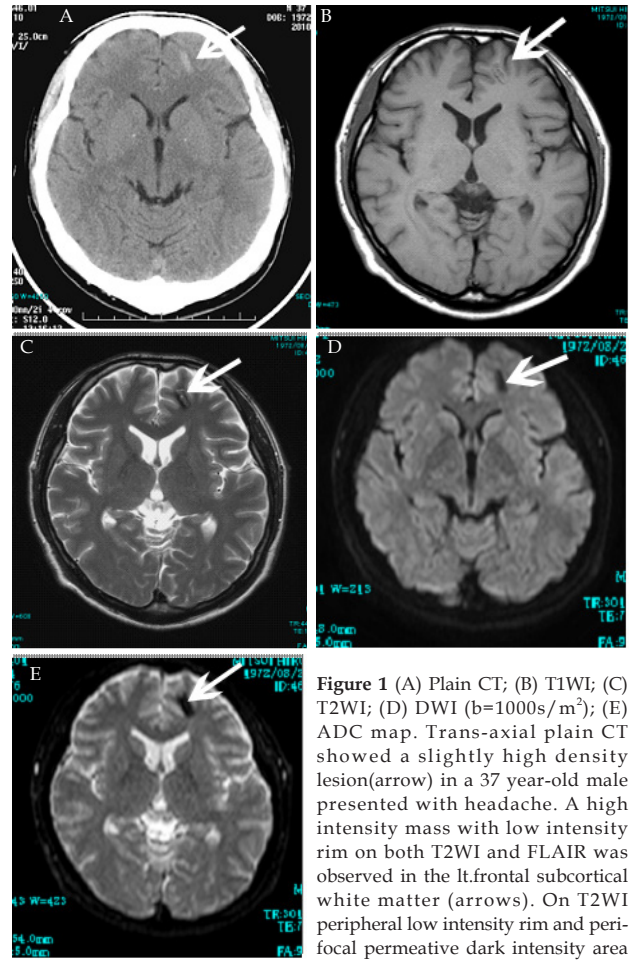


Figure 1 (A) Plain CT; (B) T1WI; (C) T2WI; (D) DWI (b=1000s/m²); (E) ADC map. Trans-axial plain CT showed a slightly high density lesion (arrow) in a 37 year-old male presented with headache. A high intensity mass with low intensity rim on both T2WI and FLAIR was observed in the lt.frontal subcortical white matter (arrows). On T2WI peripheral low intensity rim and perifocal permeative dark intensity area reflecting leakage of hemosiderin were observed in adjacent brain white matter. On Gd-enhanced T1WI, its enhancement was unclear (not shown).

Table 1 The location of CCM.

Medulla oblongata 1, medulla/pons 2, pons 3*, midbrain/pons 1, middle brain 3+, cerebellum 18, thalamus 4, internal capsule 2, basal ganglia 6+, frontal lobe 10*, parietal lobe 6, temporal lobe 6, occipital lobe 4

*: extral-lesional hemorrhage and +: intral-lesional hemorrhage were observed in each 1 case.

Table 2 The signal intensity of T1WI, T2WI, FLAIR, T2*WI and DWI. Cases (percentile).

	T1WI	T2WI	FLAIR	T2*WI	DWI
High	16 (24)	5 (7.5)	3 (4.5)	3 (4.5)	2 (7)
Low-slight high	24 (36)	4 (6)	8 (12)	10 (15)	3 (11)
Low	10 (15)	30 (45)	24 (36)	34 (52)	13 (46)
High and low mixed	16 (24)	27 (41)	31 (47)	19 (29)	10 (36)

Table 3 The MR signal intensity change of sequential stages of cerebral hemorrhage.

		-24h Hyperacute	-3day Acute	-2week Subacute	3 week-- late subacute
Central core	T1WI	iso	Iso	Iso	High
	T2WI	Iso	Low	Low	High
	DWI	high	Low	Low	High
Peripheral rim	T1WI	Iso	Iso	High	High
	T2WI	Iso	Low	High	High
	DWI	Low	Low	Iso	high
Surrounding brain parenchyma	T1WI	low	low	low	Iso
	T2WI	High	High	High	Iso/high
	DWI	Iso/high	High	Iso/high	Iso/high

The signal was decreased and unclear with residual ambiguous peripheral low signal rim after 17 days.

On CT, they exhibited low ($n=1$), iso ($n=3$), and high ($n=11$) density (Figure 1). The calcification (old clot or dystrophic calcification) were observed in 5 (33.4%) of 15 CT scanned lesions. In 32 lesions of 11 (48.4%) cases, they showed multilobular cystic round nodule or mass lesion. And uni-locular single nodular lesions were observed in 34 lesions of 19 (51.5%) cases.

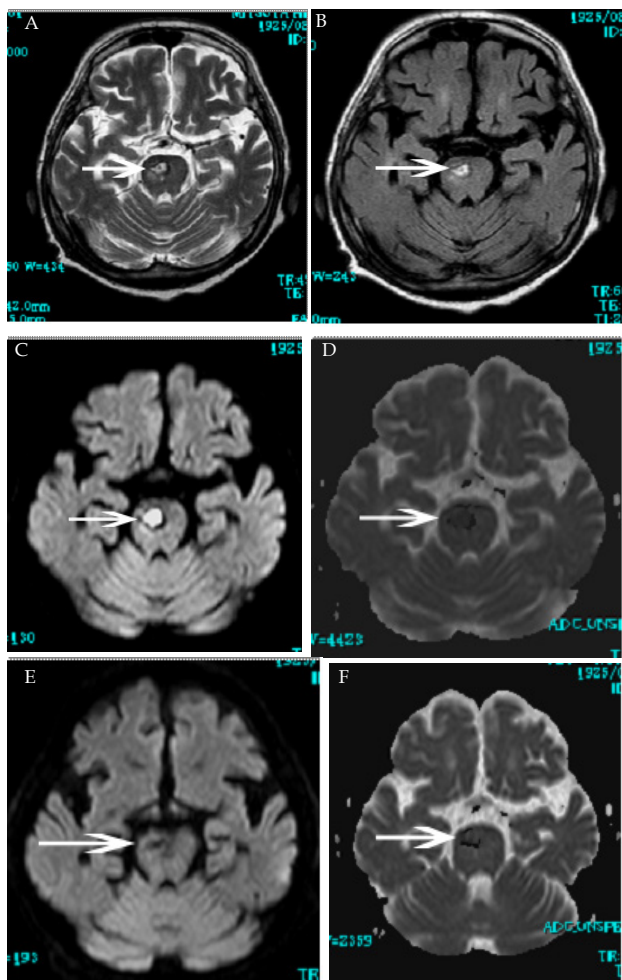


Figure 2 (A) T2WI; (B) T1WI; (C) DWI ($b=1000s/m^2$); (D) ADC map and 17 days after; (E) DWI ($b=1000s/m^2$); (F) ADC map. Transient intratumoral hemorrhage was suspected on DWI. In rt.ventral portion of pons, heterogeneously high intense lesion was observed. A 84 year-old man with double vision referred to us for the annual follow up of pontine cavernoma. The high intensity area (arrows) on both T1WI and T2WI represented a late phase of subacute hematoma. On DWI, the central core area showed very high intensity (arrow) with restriction of diffusion revealed by the ADC map. After 17 days, the signal intensity was decreased and became unclear with residual ambiguous peripheral low signal rim. On ADC map, the lesion showed slightly high signal due to the T2-shine through effect and no apparent diffusion restriction.

DISCUSSION

The cerebral cavernous malformation (CCM) is usually composed of large sinusoidal vascular spaces closely clustered together. There is no normal intervening tissue and the dilated sinusoids lack normal endothelial tight junctions. In the advent of endovascular surgery, cerebrovascular malformations have recently been reclassified according to the presence of arteriovenous shunting within the

malformation. Therefore, AVM, dural A-V fistula, vein of Galen malformation, developmental venous anomaly (DVA) (venous malformation), CCM and capillary telangiectasia are classified. The CCM was composed of dilated capillary blood vessels (angiogenically immature lesions with endothelial proliferation) and is separated by normal neural tissues. This lack of a normal endothelium readily allows leakage of blood elements. The CCM represents about 15% of all vascular malformations with an estimated incidence of about 0.1 percent (1-2). Not all CCM are associated with symptoms, but once they become symptomatic 40 to 50 percent present with seizures, 20 percent with focal neurological deficit, and 9-10 percent with hemorrhage^[1,2]. The risk of hemorrhage has been estimated between 0.2 and 2.5% per lesion per year^[3]. These numbers may be higher for patients with brain stem CCM^[4] and the symptoms may worsen when it occurs.

Most of the lesions are supratentorial in location. However, in 10-25% are infratentorial (the cerebellum or brain stem). According to the MRI study of autopsied cases, cavernoma exists in 0.4-0.7% of all subjects. They are often found in 3-5 decades and multiple CCMs are seen about 15-50% (up to 80% of affected family members) of patients^[3,5]. Familial form is inherited as an autosomal dominant trait with variable expression. The mutation of genes (CCM1-3) have been mapped at as follows; KRIT1 of CCM1 at 7q11.2-q21, malcavernin of CCM2 at 7p15-p13, PDCD10 of CCM3 at 3q26-1. The developmental venous anomaly (DVA) so called venous angioma are sometimes noted in association with cavernomas^[6]. In CCM, angiography is usually normal, although prolonged injection may demonstrate an abnormal capillary blush^[7].

CT findings consist of iso to high density area/mass and often partially calcified lesion which shows mild to moderate enhancement except the thrombosed portions. The lesion shows no mass effect or surrounding edema except when recent hemorrhage or enlargement has occurred.

The MRI appearance of cerebral cavernous malformation (CCM or cavernoma) has been well described. The typical CCM is a mixed signal lesions on all sequences encircled by a hemosiderin/ferritin rim, because they contain blood products at various stages of evolution like our study. Usually CCM shows no mass effect except rapid growth or intratumoral hemorrhage in our study because it is a kind of benign vascular hamartoma histologically. Their appearances have been described as resembling "popcorn" or "mulberries" and can be enhanced by gradient-echo imaging. The T1WI high intensity foci was occasionally observed. It was thought to reflect the extremely slow flow or stagnation or thrombosis of varying stage (mainly subacute phase). Encapsulated hematoma or resolving hematoma were also mimicking lesions on MRI images. An MRI classification for CCM has been proposed which combines the MRI findings with clinical and pathological characteristics^[10,11]. That is: type I lesions are characterized by subacute hemorrhage and exhibit a hyperintense core on T1WI (methemoglobin), whereas on T2WI the initial hyperintense signal changes to hypointensity in time with a faint hypointense rim.

The hemorrhage are ongoing in repetitive processes. The type II lesions demonstrate loculated areas of hemorrhage of varying age and thrombus surrounded by gliosis and hemosiderin. On T1 and T2WI a reticulated core with high and low signal intensities is seen surrounded by gliosis and/or hemosiderin. On T1 and T2WI a reticulated core with high and low signal intensities (Figure 2) was surrounded by a hypointense ring. Clinically these lesions are active, and thrombosis and hemorrhage are ongoing in a repetitive process. The type III lesions represent chronic mostly inactive lesions with

residual hemosiderin in and around the lesions creating hypointensity on T1 and T2WI. The type IV lesions are poorly visualized on T1 and T2 and are best seen with gradient echo sequences as small punctuate hypointense foci. Subacute hemorrhage associated with a microarteriovenous malformations or brain tumor may mimic a type I lesions, and follow-up MRI and angiography is indicated under such circumstances. The type II lesions were thought to be pathognomonic for cavernoma, but thrombosed AVM and hemorrhagic metastases may have a similar appearance^[12], type III and IV lesions may be mimicked by radiation-induced telangiectasis^[13].

T2* WI which is sensitive to inhomogeneity of magnetic field represents the apparent T2 due to dispersion of spins on the rotating frame.

Susceptibility weighted imaging (SWI) is derived from the paramagnetic susceptibility effect in order to visualize venous structures and iron in the brain and to study diverse various conditions. However, structures with higher susceptibility effect appear significantly larger than their actual size. Although, CT has proved to be more sensitive than MRI in delineating small calcified lesion besides fresh hemorrhage. Both CT and MRI can be used in the follow-up of patients with known cavernous malformation in particular when hemorrhagic events are suspected because CCM probably undergo occult hemorrhage. Thus, diffusion weighted MRI signal is helpful in predicting intratumoral bleeding (acute-subacute hemorrhage) which occur mostly within the core area as we often observed in the patients of the cerebral hemorrhage (Table 3). And the low intense signal area on T2WI assumed to reflect the hemosiderin leakage to the brain parenchyma.

Due to the magnetic susceptibility effect and deposition of deoxyhemoglobin or methemoglobin induced by slow flow in CCM they show the low signal intensity on T2*WI (BOLD: blood oxygenation level dependent) effect^[14]. T2 shortening can also be produced by hemoglobin concentration and clot retraction. Therefore, the differential diagnosis of CCM from the viewpoint of MRI signal are as follows; chronic hemorrhage, thrombosed AVM, developmental venous anomaly, hemorrhagic brain meta (renal cell carcinoma, lung cancer, melanoma etc.), amyloid angiopathy, microaneurysm or microbleed related with angitis, radiation induced cerebral hemorrhage, coagulopathy (DIC etc.), toxoplasmosis (calcified granuloma).

The low intense signal area on DWI assumed to represent the hemosiderin or susceptibility effect and blood oxygen level dependent (BOLD) effect by the deoxyhemoglobin of hematoma. Moreover there are some characteristics of its local extension; no apparent mass effect (peri-focal edema) or no apparent interval growth except hemorrhagic events. On DWI they usually showed high signal due to the highly viscosity due to change of the concentration of hemoglobin or diminishment of the extra cellular space by the regression of thrombus^[8].

However, excessive deoxyhemoglobin and methemoglobin evoke the susceptibility effect like hemosiderin. They show low signal on T2WI and T2* WI (called as T2 black out phenomenon), old hemorrhage shows very low signal on DWI and ADC map due to the effect of T2* relating hemosiderin.

The low signal area of GRE T2* weighted images and DWI is more broad than that of T2WI due to the effect of susceptibility blooming and diffusion of hemosiderin/ferritin into the adjacent brain parenchyma. The GRE images showed marked low signal by the susceptibility and blood oxygen level dependent (BOLD) effect by the deoxyhemoglobin^[16]. The deflection rate of GRE T2*WI on intracranial hemorrhage was 1.9 fold higher than that of CT, especially

in the brainstem and cerebellum where beam hardening artifact occurs on CT^[15]. As a matter of fact, we could recognize CCM more easily in DWI images than the conventional MRI scan. The transient high signal foci were observed in 2 cases that intratumoral (re) hemorrhage were suspected. So, we also think diffusion weighted MRI signal is helpful in predicting intralesional bleeding (acute-subacute hemorrhage) which mostly occur within the core area which observed in cases of cerebral hemorrhage cases in our preliminary data (Table 3).

In comparison with hypertensive hemorrhages which frequently occurs at basal ganglia, thalamus, cerebellar hemisphere, and pontine (brain stem), its locations were more diverse in CCM. And cerebral subcortical locations which are frequently observed in amyloid angiopathy were only observed in 6 (9.1%) cases in our study.

The major discriminating points between the hemorrhagic metastatic tumor such as renal cell carcinoma or melanoma are as follows; the absence of the perifocal edema and the presence of T2WI low intense rim. In addition, DWI assumes to be able to detect more easily and sensitively the hyperacute or late subacute phase of intra and/or perilesional hemorrhage as a high intensity foci than the conventional T1WI and T2WI. The limitation of this study was that: although 2 subjects were suspected of recent intratumoral hemorrhage, there were no evidence because the high signal change were diminished spontaneously. Therefore, we have to perform the DWI scan in all patients in clinical follow-up with CCM. Of course, DWI is also thought to be useful in detecting the secondary peritumoral ischemia or infarction due to the high sensitivity for the cytotoxic edema.

CONCLUSION

The cerebral cavernous malformation (CCM) shows the signal of various phase of hematoma (hemorrhage) on both T1WI and T2WI MRI. On the diffusion weighted image (DWI), they tend to show the very low signal intensity by the BOLD effect of the deoxyhemoglobin and T2 black out effect. So by using DWI, we can detect CCM more easily than the conventional MRI scan with T1WI, T2WI, FLAIR with/without T2*WI.

The low signal area of DWI is more broad than that of T2WI due to the effect of susceptibility blooming and leak of hemosiderin/ferritin into the adjacent parenchyma. The transient high signal foci were observed in 2 cases in whom intratumoral (re) hemorrhage were suspected. DWI is a useful method like T2*WI and SWI for the early detection even if they are very small and has the ability to know the occurrence of the intratumoral hemorrhage (bleeding) or the secondary infarction.

CONFLICT OF INTEREST

The author of the manuscript entitled 'The MRI Imaging of Cerebral Cavernous malformation with Practical Use of DWI (diffusion weighted image)' declare that there is no conflict of interest with regard to equipment, contrast materials.

REFERENCES

- 1 Del Curling O Jr, Kelly DL Jr, Elster AD, Craven TE. An analysis of the natural history of cavernous angiomas. *J Neurosurg.* 1991 Nov;75(5):702-8.
- 2 Zabramski JM, Wascher TM, Spetzler RF, Johnson B, Golfinos J, Drayer BP, et al. The natural history of familial cavernous malformations: results of an ongoing study. *J*

- Neurosurg.1994Mar;80(3):422-32.
- 3 Mason I, Aase JM, Orrison WW, Wicks JD, Seigel RS, Bicknell JM. Familial cavernous angiomas of the brain in a Hispanic family. *Neurology*. 1988 ;38(2):324-6.
 - 4 Porter PJ, Willinsky RA, Harper W, Wallace MC. Cerebral cavernous malformations: natural history and prognosis after clinical deterioration with or without hemorrhage. *J Neurosurg*. 1997 Aug;87(2):190-7.
 - 5 Rigamonti D, Hadley MN, Drayer BP, Johnson PC, Hoenig-Rigamonti K, Knight JT, et.al. Cerebral cavernous malformations. Incidence and familial occurrence. *N Engl J Med*. 1988 Aug 11;319(6):343-7.
 - 6 Zimmerman RS, Spetzler RF, Lee KS, Zabramski JM, Hargraves RW. Cavernous malformations of the brain stem. *J Neurosurg*. 1991Jul;75(1):32-9.
 - 7 Numaguchi Y, Kishikawa T, Fukui M, Sawada K, Kitamura K, Matsuura K, et.al. Prolonged injection angiography for diagnosing intracranial cavernous hemangiomas. *Radiology*. 1979 Apr;131(1):137-8.
 - 8 Atlas SW, DuBois P, Singer MB, Lu D. Diffusion measurements in intracranial hematomas: implications for MR imaging of acute stroke. *AJNR* 21:1190-1194, 2000.
 - 9 Silvera S, Oppenheim C, Touzé E, Ducreux D, Page P, Domigo V, et.al. Spontaneous intracerebral hematoma on diffusion-weighted images: influence of T2-shine-through and T2-blackout effects. *AJNR* 26:236-241, 2005.
 - 10 Fritschi JA, Reulen HJ, Spetzler RF. *Acta Neurochir* Cavernous malformations of the brain stem. A review of 139 cases. 1994;130(1-4):35-46.
 - 11 Rigamonti D, Drayer BP, Johnson PC, Hadley MN, Zabramski J, Spetzler RF. The MRI appearance of cavernous malformations (angiomas). *J Neurosurg*. 1987 67(4):518-24.
 - 12 Griffin C, DeLaPaz R, Enzmann D. Magnetic resonance appearance of slow flow vascular malformations of the brainstem. *Neuroradiology*. 1987;29(6):506-11.
 - 13 Gaensler EH1, Dillon WP, Edwards MS, Larson DA, Rosenau W, Wilson CB. Radiation-induced telangiectasia in the brain simulates cryptic vascular malformations at MR imaging. *Radiology*. 1994 Dec;193(3):629-36.
 - 14 Finkenzeller T, Feller FA, Trenkler J, Schreyer A, Fellner C.. Capillary telangiectasias of the pons. Does diffusion-weighted MR increase diagnostic accuracy? *Eur J Radiol*. 2010 ;74(3):e112-6.
 - 15 Liu LX, Yi HL, Han HB, Qi XM. Application of T2* measurement on gradient echo T2*-weighted imaging in differential diagnosis of intracranial hemorrhage and calcification. *Chin Med J (Engl)*. 2012 Jun;125(12):2104-8.
 - 16 De Champfleury NM, Langlois C, Ankenbrandt WJ, Le Bars E, Leroy MA, Duffau H, et.al. Magnetic resonance imaging evaluation of cerebral cavernous malformations with susceptibility-weighted imaging. *Neurosurgery*. 2011 ;68(3):641-7.

Peer reviewers: Hui-Xiong Xu, Professor, Department of Medical Ultrasound, Shanghai Tenth People's Hospital, Tenth People's Hospital of Tongji University, No. 301 Yanchangzhong Road, Shanghai, 200072, China; Lin Ma, Professor, Department of Radiology, PLA General Hospital, 28 Fuxing Road, Beijing 100853, China.